BUILDING CONSTRUCTIONS, BUILDINGS AND ENGINEERING STRUCTURES

СТРОИТЕЛЬНЫЕ КОНСТРУКЦИИ, ЗДАНИЯ И СООРУЖЕНИЯ

Check for updates

UDC 624.073+624.012+624.044

Original Empirical Research

https://doi.org/10.23947/2949–1835-2025-4-3-7-17

Determination and Analysis of Flexure $\Delta_{flexure}$ and Shear Δ_{shear} Displacements of Reinforced Concrete Walls of Civil Buildings

Oleg V. Radaikin[1,2] ✉, **Nadezhda V. Hnycheva**[2]

[1]Kazan Federal University, Kazan, Russian Federation

[2]Kazan State Power Engineering University, Kazan, Russian Federation

✉ olegxxii@mail.ru

EDN: ITESKN

Abstract

Introduction. To date, there have been extensive experimental data made available in both domestic and foreign scientific literature on the study of displacements and deformations of reinforced concrete walls under the combined action of horizontal load *Q* and vertical load *N*. However, there are not enough comprehensive works systematizing the obtained data to be used as an empirical basis for designing more accurate deformation models and engineering calculation methods for walls, allowing differentiated assessment of flexure $\Delta_{flexure}$ and shear Δ_{shear} displacements. This article aims to look into this issue.

Materials and Methods. The object of the study is reinforced concrete walls of buildings and structures under the combined action of horizontal load *Q* and vertical load *N*. The subject of the study are the displacements and deformations of the walls. Materials include scientific articles on the topic by foreign authors. The methods being used are formal logic (analysis, synthesis, induction, deduction), graphical methods for constructing deformation schemes, and analytical methods of nonlinear structural mechanics.

Research Results. For wall aspect ratios 1.5 < *H/B* < 2.0, flexure $\Delta_{flexure}$ displacements dominate in the total displacement structure Δ, while horizontal sliding displacements Δ_{slid} amount to about 1% of Δ and can be neglected. The share of flexure $\Delta_{flexure}$ is approximately 98% of Δ at the initial loading stages. As horizontal load *Q* increases, the contribution of $\Delta_{flexure}$ gradually decreases: to 90% at the moment of crack formation, to 85% at the yielding of vertical reinforcement, and to 80% at the failure stage (when compressed concrete spalls).

For wall aspect ratios 1.0 < *H/B* < 1.5, shear displacement Δ_{shear} has a significant influence on the total displacement Δ: its share at the initial loading stages is about 22%, while determining a protective concrete layer — 46%, and reaches 64% at failure.

Using the graphs of relative displacements of walls with aspect ratios 1.5 < *H/B* < 2.0, it was found that at the failure stage, the shares of flexure and shear displacements are 88% and 12% of the total, respectively. Similar graphs obtained for walls with aspect ratios 1.0 < *H/B* < 1.5 confirmed that Δ_{shear} significantly affects the total displacement Δ. The share of Δ_{shear} at initial loading is about 22%, while determining a protective concrete layer — 46%, and reaches 64% at failure.

Discussion and Conclusion. The "*X*-diagonals" method implemented in a planar calculation scheme allows for highly accurate separation of components caused by flexure and shear deformations from the total displacements. Thanks to this the scheme is a promising tool for further experimental and theoretical studies. We assume that the height of the wall segment where the diagonals are designed should be arbitrary — H_i making this method more universal.

In addition to the planar calculation scheme, a rod (beam) scheme can also be used. The rod calculation scheme of the wall, with known patterns of stiffness parameter changes in the rod end sections (at the locations of plastic hinge formation), is convenient for engineering calculations of frame buildings and structures based on the finite element method in diverse computational complexes.

Keywords: reinforced concrete, monolithic walls, experimental data, wall strength, flexure displacements, shear displacements, total displacements, flexure deformation, shear deformation, total deformation

Acknowledgments. The authors appreciate the reviewers, whose critical assessment of the submitted materials and suggestions helped to significantly improve the quality of this article.

For citation. Radaikin OV, Khnycheva NV. Determination and Analysis of Flexure $\Delta_{flexure}$ and Shear Δ_{shear} Displacements Displacements of Reinforced Concrete Walls of Civil Buildings. *Modern Trends in Construction, Urban and Territorial Planning*. 2025;4(3):7–17. https://doi.org/10.23947/2949–1835-2025-4-3-7-17

Оригинальное эмпирическое исследование

Оценка и анализ перемещений от изгиба $\Delta_{flexure}$ и сдвига Δ_{shear} железобетонных стен гражданских зданий

О.В. Радайкин[1, 2] ✉, **Н.В. Хнычева[2]**
[1] Казанский (Приволжский) федеральный университет, г. Казань, Российская Федерация
[2] Казанский государственный энергетический университет, г. Казань, Российская Федерация
✉ olegxxii@mail.ru

Аннотация
Введение. К настоящему времени в отечественной и зарубежной научной литературе накоплен обширный экспериментальный материал по исследованию перемещений и деформаций железобетонных стен при совместном действии горизонтальной Q и вертикальной N нагрузок. Однако отсутствуют обобщающие работы, систематизирующие полученные данные с целью их использования в качестве эмпирического базиса для построения более точных деформационных моделей и инженерных методик расчёта стен, позволяющих дифференцированно оценивать перемещения изгиба $\Delta_{flexure}$ и сдвига Δ_{shear}. Данная статья направлена на решение этой проблемы.

Материалы и методы. Объект исследований — железобетонные стены зданий и сооружений при совместном действии горизонтальной Q и вертикальной N нагрузок. Предмет исследований — перемещения и деформации стен. Материалы — научные статьи зарубежных авторов, посвящённые исследуемому вопросу. Методы — формальная логика (анализ, синтез, индукция, дедукция), графический метод построения схем деформирования, аналитические методы нелинейной строительной механики.

Результаты исследования. При соотношении сторон стены $1{,}5 < H/B < 2{,}0$ преобладают изгибные перемещения $\Delta_{flexure}$ в структуре общих перемещений Δ, а перемещения горизонтального скольжения Δ_{slid} составляют порядка 1 % от Δ, и ими можно пренебречь. Доля перемещений от изгиба $\Delta_{flexure}$ составляет приблизительно 98 % от Δ на начальных этапах. С увеличением горизонтальной нагрузки Q вклад перемещений $\Delta_{flexure}$ постепенно снижается: до 90 % — в момент появления трещин, до 85 % — при текучести вертикальной арматуры и до 80 % — в стадии разрушения (при выкрашивании сжатого бетона).

При соотношении сторон стены $1{,}0 < H/B < 1{,}5$ перемещение Δ_{shear} оказывает значительное влияние на общее перемещение Δ: доля Δ_{shear} на начальных этапах нагружения составляет около 22 %, в момент отслоения защитного слоя бетона — 46 %, и достигает 64 % в момент разрушения.

По графикам относительных перемещений стены при соотношении сторон $1{,}5 < H/B < 2{,}0$ нами выявлено, что в стадии разрушения доля перемещений при изгибе и сдвиге составляет соответственно 88 % и 12 % от общих. Аналогичные графики получены для стен с соотношением сторон $1{,}0 < H/B < 1{,}5$ и установлено, что перемещение Δ_{shear} оказывает значительное влияние на общее перемещение Δ. Доля Δ_{shear} на начальных этапах нагружения составляет около 22 %, в момент отслоения защитного слоя бетона — 46 % и достигает 64 % в момент разрушения.

Обсуждение и заключение. Метод «X-диагоналей», реализованный в плоской расчётной схеме, позволяет с высокой точностью выделить из общих перемещений составляющие, вызванные деформациями изгиба и сдвига. Благодаря этому преимуществу, данная схема является перспективным инструментом для дальнейших экспериментальных и теоретических исследований. Причём, на наш взгляд, высота фрагмента стены, в границах которого строятся диагонали, должна быть произвольной — H_i, что позволит сделать данный метод более универсальным.

Помимо плоской расчётной схемы возможно использование и стержневой. Стержневую расчётную схему стены при известных закономерностях об изменениях жесткостных параметров стержня на концевых участках (в местах образования пластических шарниров) удобно применять в инженерных расчётах каркасных зданий и сооружений на основе метода конечных элементов в том или ином вычислительном комплексе.

Ключевые слова: железобетон, монолитные стены, экспериментальные данные, прочность стены, перемещения при изгибе, перемещения при сдвиге, общие перемещения, деформация при изгибе, деформация при сдвиге, общая деформация

Благодарности. Авторы выражают благодарность редакции и рецензентам за внимательное отношение к статье и указанные замечания, которые позволили повысить ее качество.

Для цитирования. Радайкин О.В., Хнычева Н.В. Оценка и анализ перемещений от изгиба $\Delta_{flexure}$ и сдвига Δ_{shear} железобетонных стен гражданских зданий. *Современные тенденции в строительстве, градостроительстве и планировке территорий*. 2025;4(3):7–17. https://doi.org/10.23947/2949–1835-2025-4-3-7-17

Introduction. Reinforced concrete walls are among the most common types of building structures. They typically combine load-bearing and enclosing functions, experience vertical and horizontal loads, and thereby operate under conditions of complex stress-strain states. An accurate assessment of the deformations occurring during the process is key to their precise mechanical calculation and further safe operation. This paper looks into the movements and deformations of walls.

Before moving on with the study description, let us get clear on the terminology:

– movement is a change in the coordinates of a point of a solid body (in our casea reinforced concrete wall) in space under the action of loads (external forces) denoted by the Greek letter Δ_{index} with its lower index showing the nature of the influence of deformations of the solid body, such as flexure, shear, sliding, etc.;

– deformation is a change in the size and shape of a solid body under the action of a load, i.e., it is the mutual displacement of points of a solid body relative to each other in space. Linear relative deformations — ε, shear angles — γ, angles of rotation of sections of the solid body relative to its axes — φ, and the curvature of the axes themselves — χ (*note:* they are commonly denoted as 1/ρ in literature).

The total displacement of any point of a reinforced concrete wall due to loads acting in its plane can be broken down into the following components:

$$\Delta = \Delta_{flexure} + \Delta_{shear} + \Delta_{slid} + \Delta_{BR}, \tag{1}$$

where $\Delta_{flexure}$ — displacements caused by the influence of pure flexure deformations; Δ_{shear} — displacements caused by the influence of pure shear deformations in the plane of the wall; Δ_{slid} — displacements caused by the influence of sliding-shear deformations at the bottom or the top of the wall; Δ_{BR} — displacements caused by the influence of the rotation of the bottom or top of the wall relative to the foundation or floor.

Having studied the scientific and technical literature analyzed below, we have identified the following problem: there are no comprehensive studies systematizing the experimental data (accumulated considerably over the past few decades) on the deformation of reinforced concrete walls under the combined action of horizontal, *Q*, and vertical, *N*, loads. This serves as an obstacle both for improving the existing methods and techniques for the differentiated calculation of flexure $\Delta_{flexure}$ and shear Δ_{shear} displacements of reinforced concrete walls, as well as for coming up with fundamentally new approaches. The current studying is aimed at addressing this obstacle.

The movements caused by loads acting out of the plane of the wall are beyond the scope of the research.

Materials and Methods. Prevously in [1], we described the general mechanisms of deformation and failure of walls under the combined influence of the load ratio *N/Q* and the height-to-width ratio of the wall — *H/B*. It was found that the ratio *H/B* qualitatively predetermines the wall failure mechanism, i.e., it impacts the pattern of appearance and development of cracks from a microscopic size to major ones, along the trajectory of which the wall structure is divided into separate parts. The load ratio *N/Q* is responsible for the quantitative values of the parameters of implementing this mechanism. At small values of *H/B*, the share of shear displacements Δ_{shear} predominates in the resulting displacements of the wall Δ, while the resistance to horizontal load *Qu* is at its maximum. In this case, the failure is more brittle in its nature. As the ratio *H/B* increases, so does the share of the flexure displacements $\Delta_{flexure}$, while the shear displacements Δ_{shear} decrease; so does Q_u, and plastic deformations are more intense.

The mechanisms of deformation and failure of walls under load described in [1] enable one to design deformed schemes with the overlay of internal force schemes balancing external loads. These deformed schemes allow us to calculate the total displacements of the wall Δ at its characteristic sections, and most importantly, to isolate the components caused by the influence of flexure and shear deformations — $\Delta_{flexure}$ and Δ_{shear} respectively — from the total displacements. Some variants of such schemes by different authors are considered below, along with their analysis regarding the correspondence of each to a relevant study of wall structures and their convenience as a tool for analyzing the stress-strain state of walls.

Research Results. One of such schemes is found in [2, 3]. Given some necessary additions made for a more complete 9nderstanding, it is shown in Fig. 1.

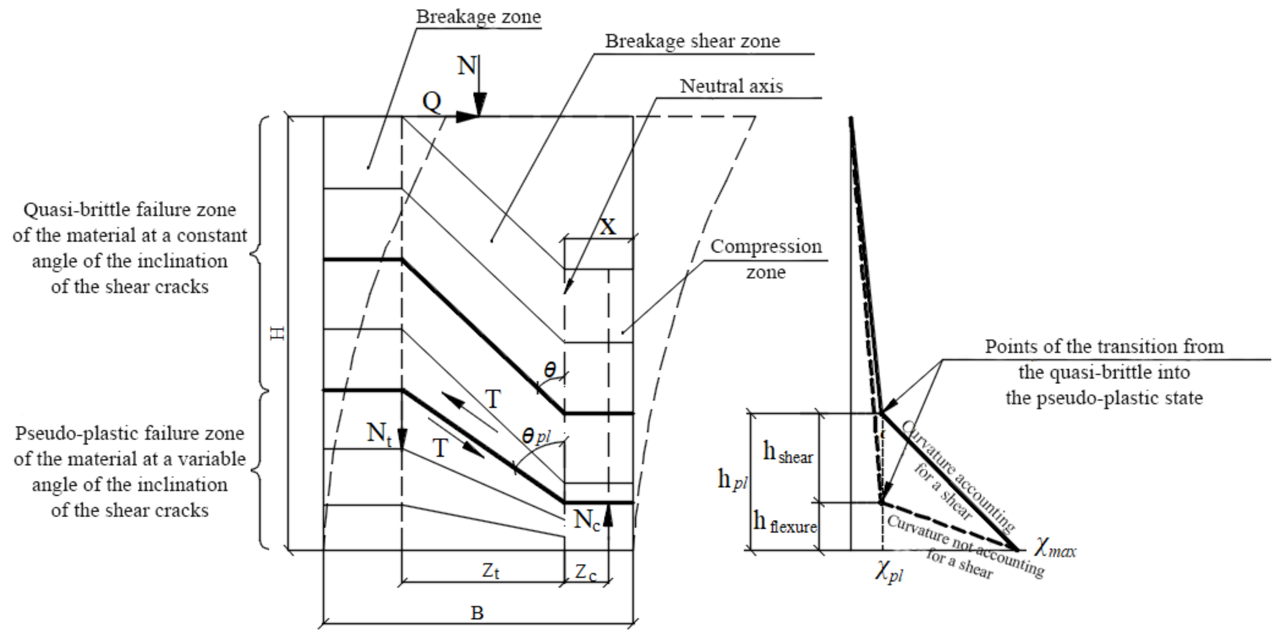

Fig. 1. Calculation scheme of deformation of a reinforced concrete wall (left) under the combined action of vertical *N* and horizontal *Q* loads and the graph of curvature distribution along its height (right) [2]

The scheme is a rectangular plate with a clamped lower edge, while all of the other three edges are free from constraints. A vertical load *N* and a horizontal load *Q* are applied from above. A pattern of fan-shaped cracks is drawn on the plate whose nature was revealed during the experiment. Along the trajectory of one of the cracks, a calculated section is drawn, i.e., the first thick line from the bottom. It intersects on the left with the stretched zone of the wall, or the detachment zone, where the detachment mechanism of crack formation dominates; in the center is the zone of combined shear and detachment where two mechanisms of crack formation overlap, i.e., transverse detachment and longitudinal shear; on the right is the compression zone of the wall. The stable development of cracks occurs largely due to the dissipation of accumulated energy from elastic-plastic deformation of pure flexure causing displacements $\Delta_{flexure}$, while shear or sliding deformations causing displacements Δ_{shear} and Δ_{slid} result in spontaneous cracking and almost instantaneous brittle failure in the local zone.

On the right in Fig. 1 are the theoretical curvature diagrams of the neutral axis of the wall. The solid line corresponds to the total curvature defined by the combined consideration of flexure and shear deformations, while the dashed line corresponds only to flexure with no shear. Each diagram consists of two straight lines with different slopes: in the lower part of the wall, the angle is softer, accordingly, the curvature changes more intensively in the height than at the top. The point of inflection between these sections corresponds to the transition from a quasi-brittle failure mechanism at the top of the wall to a pseudo-plastic failure mechanism at the bottom of the wall. Along the broken line of the cross-section of the wall, a system of internal forces is applied: N_c — the resultant compressive stresses in the concrete; N_t — the resultant tensile stresses in the concrete; T — the resultant shear stresses along the edges of the inclined crack. Fig. 1 also denotes $h_{flexure}$, h_{pl} — the height of the pseudoplastic failure zone at the bottom of the wall, respectively, assuming that there are only pure flexure deformations, and while accounting for a combination of flexure and shear deformations; χ_{pl} — the curvature corresponding to the height h_{pl}; χ_{max} — the maximum curvature; x — the height of the compressed zone; z_c — the arm of the resultant N_c relative to the neutral axis; z_t — the arm of the resultant N_t also relative to the neutral axis; θ, θ_{pl} — the angle of inclination of the cracks forming according to the pull-shear mechanism, respectively, in the upper zone of the wall (above the point of transition from quasi-brittle failure to pseudoplastic) and in the lower zone (below this point), with θ — const and θ_{pl} — *var*.

It should be noted that the resultant tensile stresses N_t in the calculated section is located above the resultant compressive stresses N_c precisely due to the influence of shear deformations. In pure flexure these forces would be at the same horizontal level.

The angle of inclination of the cracks θ_{pl} at the transition point is given by the formula:

$$\theta_{pl} = arctg\left(\frac{z_t}{h_{shear}}\right). \tag{2}$$

where $h_{shear} = h_{pl} - h_{flexure}$.

According to the experiment [2], the value of θ_{pl} ranges from 55° to 65°.

In Fig. 2, the curvature diagrams of the neutral axis of the wall are shown [2]: two theoretical ones — the first under the assumption of deformations only due to flexure (1), the second — accounting for both flexure and shear (2), as well as the experimental diagram (3) described (approximated) by the previous two theoretical diagrams.

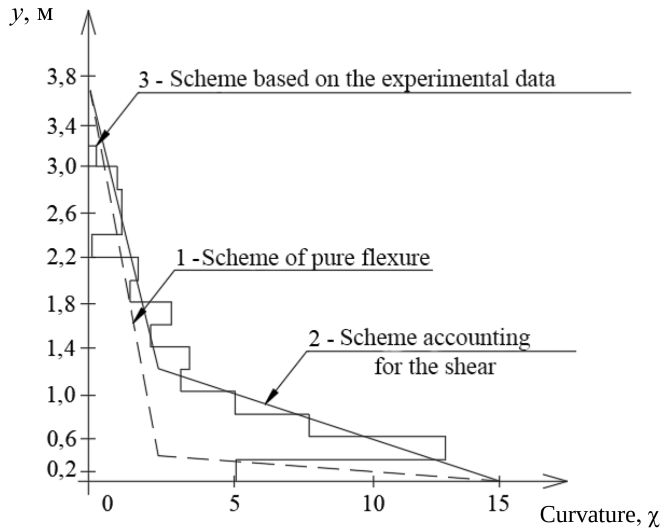

Fig. 2. Curvature distribution schemes along the wall height [2]

The maximum difference between diagrams 1 and 2 was 31%, which is significant.

In order to calculate the components of deformations and displacements caused by flexure and shear separately, some general clarifications will be introduced into the calculation scheme (Fig. 1) and moved to the scheme (Fig. 3) [4]:

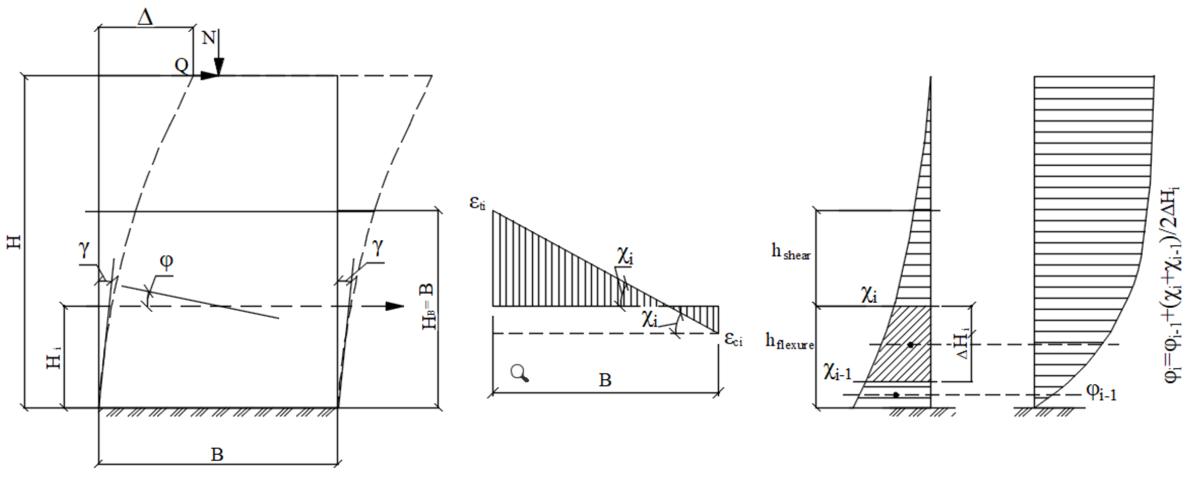

a) *b)* *c)* *d)*

Fig. 3. Calculation schemes for determining shear angles, γ, longitudinal relative deformations, ε, curvatures, χ, and rotation angles, φ, while deforming a wall: *a* — scheme of wall deformation; *b* — diagram of the distribution of longitudinal deformations ε in an arbitrary i-th section of the wall drawn at a height H_i from the base; *c* — diagram of the distribution of curvature along the height of the wall; *d* — diagram of the distribution of rotation angles [4]

In order to assess the bending deformations, let us look at the curvature diagram in Fig. 3B described by some continuous and differentiable function $\chi = \chi(y)$. Let i be the ordinal number of an arbitrary cross-section of the wall located at a height H_i from its bottom. In this section, the diagram of relative deformations ε of the wall is shown in Fig. 3A whose extreme values are related to the curvature known from the strength of materials formula:

$$\chi_i = \frac{|\varepsilon_{ti}| + |\varepsilon_{ci}|}{B}, \tag{3}$$

where ε_{ti} and ε_{ci} — deformations of tension and compression on the side faces of the wall width B.

The average value of the curvature on a wall section with a height of ΔH_i enclosed between two close sections i and i–1 is $(\chi_i + \chi_{i-1})/2$. Then the angle of rotation of the wall cross-section at the level of the center of gravity of the section ΔH_i (Fig. 3*d*) is given by the formula:

$$\varphi_i = \int_0^{H_i} \chi(y)dy = \frac{\varphi_{i-1} + (\chi_i + \chi_{i-1})}{2\Delta H_i}. \tag{4}$$

The desired displacements in an arbitrary *i*-th section are given by the formulas:

$$\Delta_{flexure,i} = \varphi_i H_i, \tag{5}$$

$$\Delta_{shear,i} = \gamma_i H_i, \tag{6}$$

where γ_i — the angle of displacement of the wall face at a height from the base (Fig. 3 *a*).

Determining the relative deformations ε_{ti} and ε_{ci} of the vertical wall faces during the experiment appears to be not challenging. To this end, the methods such as strain gauges, holographic interferometry, etc. can be used. It is thus fairly simple to estimate the movements of pure flexure $\Delta_{flexure}$ with formulas (3)-(5). However, the pure shear disp Δ_{shear} are more challenging [5].

In [4, 6-8], the computational method of "*X*-diagonals" is set forth in order to estimate these displacements (Fig. 4). To this end, the authors selected a square fragment of the wall with a width *B* and a height $H_b = B$. But we believe that the height of the fragment can be arbitrary, i.e., H_i, which will make this method more universal.

The desired displacement of the shift Δ_{shear} is estimated by changing the lengths of the diagonals of the selected square before *(d)* and after deformation (d_1', d_2') (Fig. 4 *a*):

$$\Delta_{shear} = \gamma H_B = \left(\frac{d}{2B}\right)(d_1^{'} - d)d - (d_2^{'} - d)H_B. \tag{7}$$

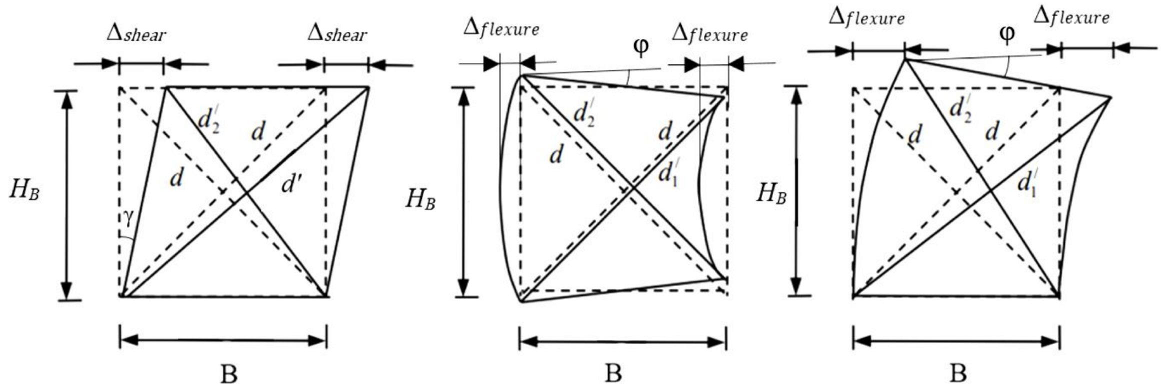

a) *b*) *c*)

Fig. 4. Geometric schemes of wall deformation for determining flexure $\Delta flexure$ and shear $\Delta shear$: a — scheme of pure flexure; b — scheme of pure flexure with a constant curvature along the height; c — scheme of pure flexure with a variable curvature along the height [4, 7]

Formula (7) is accurate only if the curvature of the deformed wall faces is constant in height (Fig. 4*b*). This is possible in some small (infinitesimal) area, in other cases it results in noticeable errors. The estimate of the shear displacement Δ_{shear} in this case turns out to be overestimated as it also contains flexure displacements $\Delta_{flexure}$ (Fig. 4 *c*).

In order to clarify formula (7), let us consider the wall deformation scheme in Fig. 5 accounting for vertical displacements.

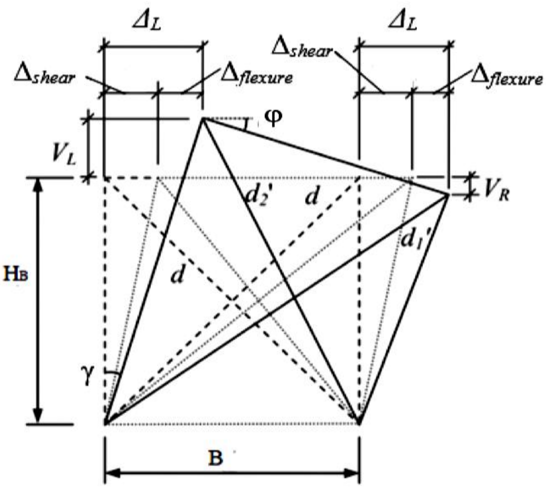

Fig. 5. Flexure $\Delta_{flexure}$ and shear Δ_{shear} displacements accounting for vertical displacements V_L and V_R [4, 7]

The flexure displacements and the angle of rotation of the horizontal section of the wall φ are equal to:

$$\Delta_{flexure} = \alpha\varphi H_B, \tag{8}$$

$$\varphi = \frac{V_L - V_R}{L}, \tag{9}$$

where V_L and V_R — vertical displacements of the upper face of the wall on the left and right sides, respectively; α — coefficient accounting for a change in the curvature along the height of the wall given by the formula (for a graphical interpretation of the coefficient, see Fig. 6):

$$\alpha = \frac{\int_0^H \varphi(y)dy}{\varphi H}. \tag{10}$$

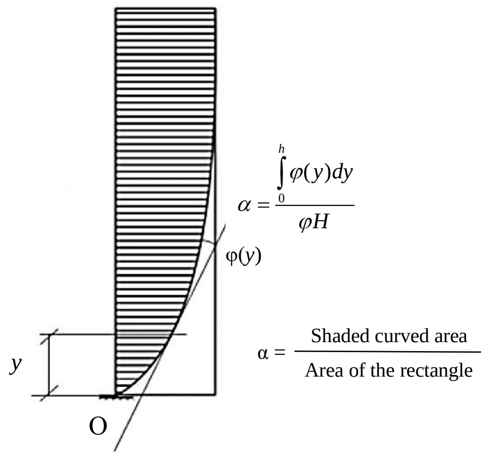

Fig. 6. Scheme of the distribution of the angles of rotation of the curved wall face after deformation for determining the coefficient α [4, 7]

This coefficient ranges within 0.5 < α < 1.0 and averages α ≈ 0.62. The values of α close to the boundaries of the interval (0.5; 1.0) are an idealized abstraction which can be used in theoretical models for simplification, but they are not implemented in practice. The essence of the coefficient is that the greater α, the more flexible the wall structure is, i.e., the lower its flexure stiffness is. Conversely, the lower the α, the higher the bending resistance of the wall structure is, i.e., the higher its flexure stiffness is.

The specified shear displacements are equal to:

$$\Delta_{shear} = \left(\frac{d}{2B}\right)\left[(d_1' - d) - (d_2' - d)\right] - \left[\Delta_{flexure} + \left(\frac{H_B}{2B}\right)(V_R - V_L)\right] \tag{11}$$

or

$$\Delta_{shear} = \left(\frac{d}{2B}\right)\left[(d_1' - d) - (d_2' - d)\right] - (\alpha - 0,5)\varphi H. \tag{12}$$

Hence in order to obtain the contribution of flexure $\Delta_{flexure}$ and shear Δ_{shear} displacements to the total displacements, it is necessary to determine the coefficient α accounting for a change in the curvature over the height of the wall. Moreover, at α = 0.5, formula (12) is reduced to (7), i.e., in this case, the gradient of the flexure curvature no longer impacts the shear.

The experimental results [4, 7] showed that before cracks are formed, the curvature of the walls has an almost constant height distribution, respectively, the coefficient α ≈ 0.5. As cracks appear, the plot of the curvature distribution becomes triangular, and the coefficient α increases to about 0.67. As the load further increases, so does α and tends to 1.0 at the moment of failure, which is accompanied first by the shutdown of the vertical reinforcement and then by the discoloration of the compressed concrete.

It was also found that as the wall aspect ratio *H/B* increases, the value of α decreases.

[9] provides a core model for calculating the wall accounting for the compliance of the supporting nodes *A* and *B* (Fig. 7) under the combined action of longitudinal *N* and transverse *Q* forces. Initially, the scheme was used to calculate columns, but in this case it is used to model reinforced concrete walls with an aspect ratio of 1.5 < *H/B* < 2.0 in order to obtain flexure $\Delta_{flexure}$ and shear Δ_{shear} displacements separately.

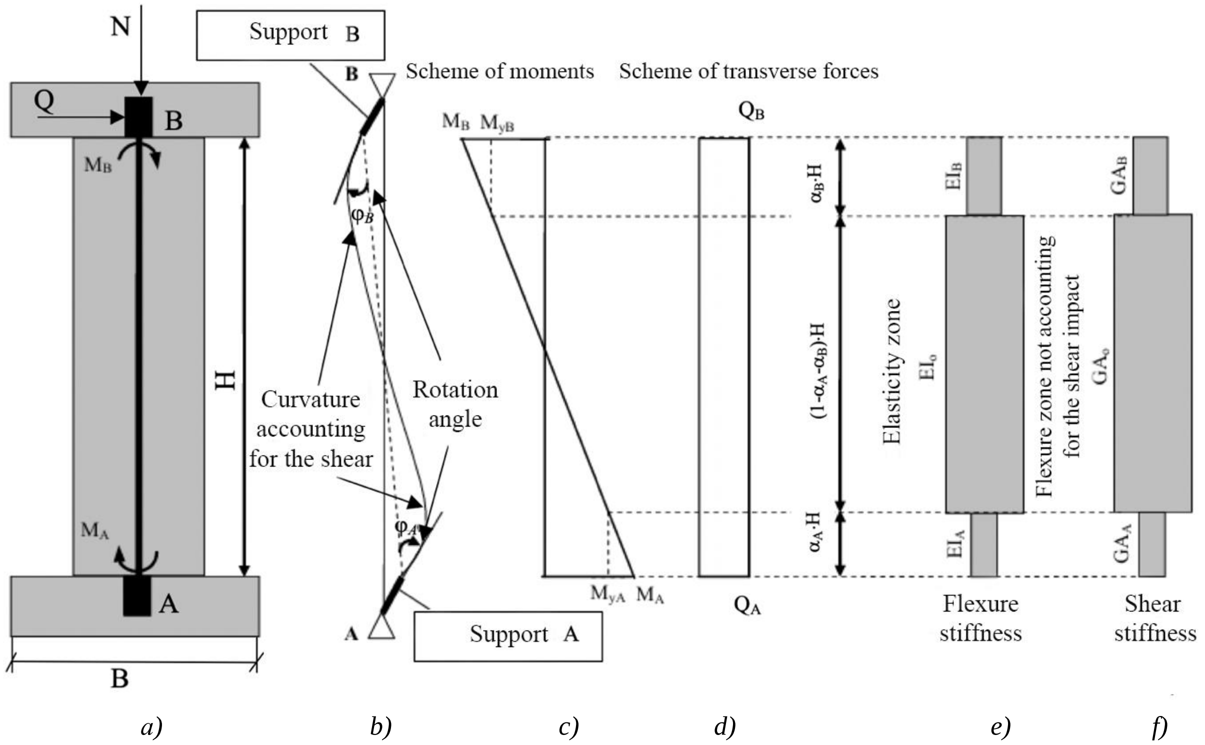

Fig. 7. Core design scheme for deforming a reinforced concrete wall under the combined action of vertical *N* and horizontal *Q* loads: *a* — core model for calculating the wall; *b* — scheme for bending the longitudinal axis of the rod during deformation; *c* — plot of moments; *d* — plot of transverse forces; *e* — scheme for modeling wall flexure; *f* — scheme for modeling walls accounting for the interaction of shear and flexure [9]

The scheme consists of a rod pinched in the upper and lower parts at points *A* and *B* (Fig. 7*a*). The rod deformation scheme is shown in Fig. 7*b*. In Fig. 7*c* in and Fig. 7*d* are the schemes of moments and transverse forces, respectively.

In order to determine the curvature of the longitudinal axis of the flexure rod $\chi_{flexure}$ caused by flexure, the distribution of bending stiffness *EI* over the height of the wall is shown in Fig. 7*d*. In order to determine the curvature of the axis of the χ_{shear} rod caused by shear, the distribution of shear stiffness *GA* over the height of the wall is shown in Fig. 7*e*. At the ends of the rod, for one and the other stiffness, it is assumed that the physical nonlinearity of reinforced concrete is accounted for (the stiffness of EI_A and EI_B, GA_A and GA_B in Figs). In the middle part of the rod, the stiffness is assumed as for an elastic body (stiffness EI_0, GA_0). At the same time, a constant value is assumed for each of the three stiffness sections.

The lengths of the end sections of the rod within which physical nonlinearity is accounted for, are determined by multiplying the height of the wall *H* by the empirical coefficients α_A and α_B. The points separating the end sections from the middle are plastic hinges.

The shear displacements Δ_{shear} acquire noticeable values at the end sections of the rod, they practically do not appear in the middle part and the movements $\Delta_{flexure\text{c}}$ caused by flexure dominate.

The total displacement of the wall Δ in the area of the plastic hinge is equal to:

$$\Delta = \Delta_{shear} + \Delta_{flexure} \tag{13}$$

The studies [6–7, 10–12] consider examine pure flexure $\Delta_{flexure}$ and shear displacements Δ_{shear} as part of the total displacement Δ with a wall aspect ratio of $1.5 < H/B < 2.0$. It is shown that flexure displacements $\Delta_{flexure}$ dominate in such walls, and sliding displacements Δ_{slid} are on the order of 1% of Δ and can be ignored. The proportion of movements from bending is approximately 98% of the total movement of the reinforced concrete wall at the initial stages. As the horizontal load *Q* increased, the contribution of movements from bending $\Delta_{flexure}$ gradually decreased to 90% at the moment of cracking; 85% — during the fluidity of vertical reinforcement; 80% — at the stage of failure (while painting compressed concrete).

According to the results of processing experiments [6, 7], graphs of relative wall movements with an aspect ratio of $1.5 < H/B < 2.0$ were obtained as shown in Fig. 8 *a*. It can be seen that at the failurre stage, the proportion of flexure and shear displacements is 88% and 12% of the total, respectively.

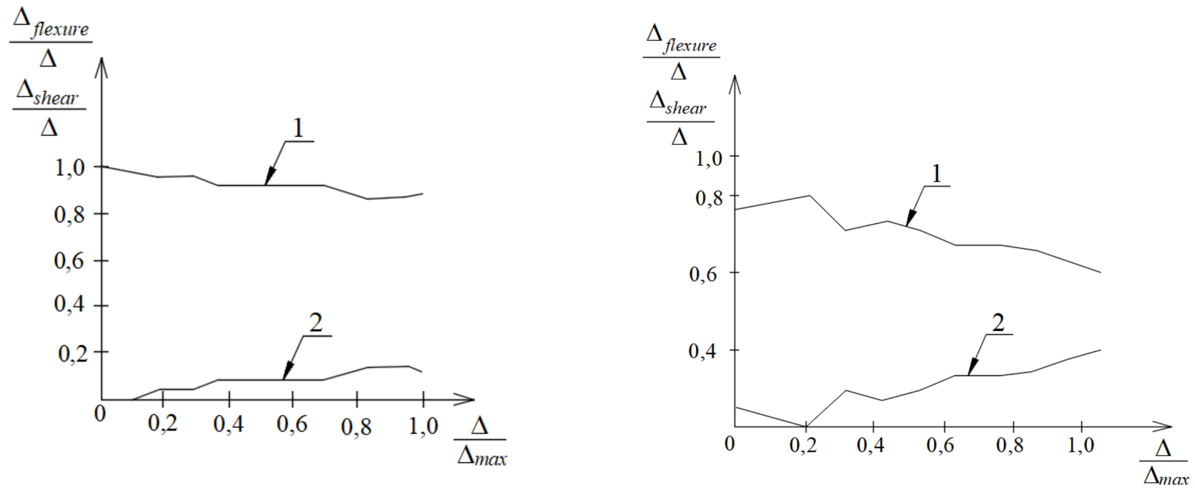

a) *b*)

Fig. 8. Graphs of relative wall displacements with the aspect ratio: *a* — 1,5 < *H/B* < 2,0; *b* — 1,0 < *H/B* < 1,5 (1 — curve of relative flexure displacements $\Delta_{flexure}/\Delta_{max}$; 2 — curve of relative shear displacements $\Delta_{shear}/\Delta_{max}$; Δ_{max} — maximum wall displacements)

We obtained similar graphs after processing the data [6] (Fig. 8*b*) for walls with an aspect ratio of 1.0 < *H/B* < 1.5. It has been found that the shear displacement Δ_{shear} has a significant impact on the overall movement of Δ. The proportion of Δ_{shear} at the initial stages of loading is about 22%, at the moment of detachment of the protective layer of concrete — 46% and reaches 64% at the moment of failure.

In an experiment [6] it was shown that at the initial stages of loading, slight displacements $\Delta_{flexure}$ are observed in the samples (Fig. 9*a*). As the first crack appears, the bending stiffness of the wall decreases sharply leading to a significant increase in the displacements $\Delta_{flexure}$.

Fig. 9*b* shows that as the first inclined crack appears, the displacements Δ_{shear} start having a more significant effect on the total wall displacements Δ, despite the fact that the shear strength of the walls is more than 2 times higher than the horizontal load *Q*.

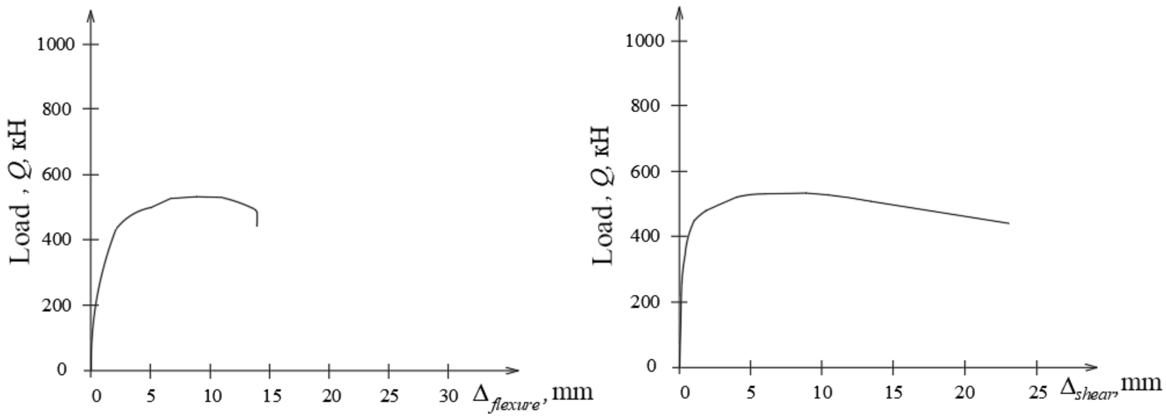

a) *b)*

Fig. 9. Graphs of the dependence of the flexure $\Delta_{flexure}$ (*a*) and shear Δ_{shear} (*b*) displacements of the wall on the applied horizontal load *Q* [6]

Discussion and Conclusion. The mechanisms of deformation and failure of walls under load identified in the experiments conducted by a wide range of foreign authors enabled us to design appropriate deformation schemes with the superposition of internal forces balancing external loads. This made it possible to obtain mathematical formulas for determining the total displacements of the wall Δ in its characteristic sections, as well as dependencies that allow the components caused by the influence of flexure and shear deformations $\Delta_{flexure}$ and Δ_{shear} to be isolated from the total displacements.

The scheme in Fig. 1 enables us to determine the desired displacement of shear Δ_{shear} and flexure $\Delta_{flexure}$ under the combined action of vertical, *N*, and horizontal, *Q*, loads. Theoretical diagrams of the curvature of the neutral axis of the wall are provided where a solid line corresponds to the total curvature determined by accounting for a combination of flexure and shear deformations, and a dotted line corresponds only when flexure without shear is accounted for. It is found that the maximum difference between the pure bending and shear-adjusted plots is 31% indicating that the calculation of walls using the model of an uncenterically compressed rod without accounting for shear displacements will have a significant error.

The scheme in Fig. 3 enables us to calculate the components of deformations and displacements caused by bending and shear separately, but with some generalizing refinements. Pure flexure displacements $\Delta_{flexure}$ are determined by means of fairly simple formulas, but pure shear displacements Δ_{shear} are challenging. In order to estimate these displacements, the computational method of "*X*-diagonals" is set forth. However, in order to obtain the contribution of flexure $\Delta_{flexure}$ and shear Δ_{shear} displacements to the total displacements, it is necessary to perform arithmetically complex operations to find the coefficient α accounting for a change in the curvature along the height of the wall.

Initially the scheme in Fig. 7 was used for calculating columns, but in this case it is used for modeling reinforced concrete walls with an aspect ratio of $1.5 < H/B < 2.0$ in order to obtain flexure $\Delta_{flexure}$ and shear Δ_{shear} displacements. In order to implement this scheme in a computing complex, it is required that conduct large-scale experimental and theoretical studies are performed on more complex (more precise) wall models.

As a result of the theoretical study, it was found that the scheme shown in Fig. 1 provides a more precise description of the wall structure and can be used as a practical tool in order to analyze its stress-strain state under the combined action of vertical force *N* and horizontal force *Q*.

References

1. Radaykin OV, Khnycheva NV Influence of Various Factors on the Strength, Rigidity and Crack Resistance of Monolithic Reinforced Concrete Walls of Civil Buildings: Classification of Factors, Influence of Geometric Parameters and Load Ratios. *Engineering Journal of Don.* 2024;11. (In Russ.) URL: http://www.ivdon.ru/ru/magazine/archive/n11y2024/9634 (accessed: 08.06.2025).

2. Schuler H Flexural and Shear Deformation of Basement-Clamped Reinforced Concrete Shear Walls. *Materials.* 2024;17(10):2267. https://doi.org/10.3390/ma17102267

3. Schuler H, Meier F, Trost B Influence of the Tension Shift Effect on the Force–Displacement Curve of Reinforced Concrete Shear Walls. *Engineering Structures*. 2023;274:115144. https://doi.org/10.1016/j.engstruct.2022.115144

4. Mohamed N, Farghaly AS, Benmokrane B, Neale KW Flexure and Shear Deformation of GFRP-Reinforced Shear Walls. *Journal of Composites for Construction*. 2013;18(2). https://doi.org/10.1061/(ASCE)CC.1943-5614.0000444

5. Massone LM, Orakcal K, Wallace JW Shear-Flexure Interaction for Structural Walls. In book: *SP-236, ACI Special Publication — Deformation Capacity and Shear Strength of Reinforced Concrete Members Under Cyclic Loading*. 2006. P. 127–150. URL: https://www.researchgate.net/publication/284079633 (accessed: 08.06.2025).

6. Mohamed N *Strength and Drift Capacity of Gfrp-Reinforced Concrete Shear Walls.* Canada: University of Sherbrooke; 2013. 155 p. URL: https://www.academia.edu/79574653/Strength_and_Drift_Capacity_of_Gfrp_Reinforced_Concrete_Shear_Walls (accessed: 08.06.2025).

7. Arafa A *Assessment of Strength, Stiffness and Deformation Capacity of Concrete Squat Walls Reinforced with GFRP Bar.* Canada: Sohag University; 2017. 223 p. https://doi.org/10.13140/RG.2.2.16345.06245

8. Kolozvari KI *Analytical Modeling of Cyclic Shear — Flexure Interaction in Reinforced Concrete Structural Walls.* Los Angeles: University of California; 2013. 334 p. URL: https://escholarship.org/uc/item/6sm78634 (accessed: 08.06.2025).

9. Mergos PE, Beyer K Modelling Shear-Flexure Interaction in Equivalent Frame Models of Slender RC Walls. *The Structural Design of Tall and Special Buildings*. 2013; 23(15):1171–1189. https://doi.org/10.1002/tal.1114

10. Hiraishi H Evaluation of Shear and Flexural Deformations of Flexural Type Shear Walls. *Bulletin of the New Zealand National society for Earthquake Engineering*. 1984;17(2):135–144. https://doi.org/10.5459/bnzsee.17.2.135-144

11. Beyer K, Dazio A, Priestley MJN Shear Deformations of Slender Reinforced Concrete Walls under Seismic Loading. *ACI Structural Journal*. 2011;108(2):167–177. URL: https://www.researchgate.net/publication/286384751 (accessed: 08.06.2025).

12. Mohamed N, Farghaly AS, Benmokrane B, Neale KW Experimental Investigation of Concrete Shear Walls Reinforced with Glass-Fiber-Reinforced Bars under Lateral Cyclic Loading. *Journal of Composites for Construction*. 2014;18(3). https://doi.org/10.1061/(ASCE)CC.1943-5614.0000393

About the Authors:

Oleg V. Radaikin, D.Sci. (Eng.), Professor of the Department of Energy Supply of Enterprises, Construction of Buildings and Structures, Kazan State Power University (51 Krasnoselskaya Str., Kazan, 420066, Russian Federation), Associate Professor of the Department of Structural and Design Engineering, Kazan (Volga Region) Federal University (18/1 Kremlevskaya Str., Kazan, 420008, Russian Federation), ORCID, olegxxii@mail.ru

Nadezhda V. Khnycheva, PhD Student, Department of Energy Supply of Enterprises, Construction of Buildings and Structures, Kazan State Power Engineering University (51 Krasnoselskaya Str., Kazan, 420066, Russian Federation), ORCID, vartsk@gmail.com

Claimed contributorship:
OV Radaikin: development of the idea, aims and objectives of the study
NV Khnycheva: data collection, analysis and interpretation, manuscript preparation.

Conflict of interest statement: **the authors do not have any conflict of interest.**

All authors have read and approved the final version of manuscript.

Об авторах

Радайкин Олег Валерьевич, доктор технических наук, профессор кафедры энергообеспечения предприятий, строительства зданий и сооружений Казанского государственного энергетического университета (420066, Российская Федерация, г. Казань, ул. Красносельская, 51), доцент кафедры конструктивно-дизайнерского проектирования Казанского (Приволжского) федерального университета (420008, Российская Федерация, г. Казань, ул. Кремлевская, 18/1), ORCID, olegxxii@mail.ru

Хнычева Надежда Вячеславовна, аспирант кафедры энергообеспечения предприятий, строительства зданий и сооружений Казанского государственного энергетического университета (420066, Российская Федерация, г. Казань, ул. Красносельская, 51), ORCID, vartsk@gmail.com

Заявленный вклад авторов:
О.В. Радайкин: формирование идеи, формулировка цели и ключевых задач.
Н.В. Хнычева: сбор данных, их анализ и интерпретация, оформление.

Конфликт интересов: **авторы заявляют об отсутствии конфликта интересов.**

Все авторы прочитали и одобрили окончательный вариант рукописи.

Received / Поступила в редакцию 05.07.2025
Revised / Поступила после рецензирования 20.07.2025
Accepted / Принята к публикации 05.08.2025